Research Article
Vol. 25, No. 22 | 30 Oct 2017 | OPTICS EXPRESS 27086
Optics EXPRESS

# New theoretical formulation for the determination of radiance transmittance at the water-air interface

**PRAVIN JEBA DEV AND PALANISAMY SHANMUGAM***

*Ocean Optics and Imaging Laboratory, Department of Ocean Engineering, Indian Institute of Technology Madras, Chennai - 600036, India*
**pshanmugam@iitm.ac.in*

**Abstract:** Radiative transfer across the water-air interface has important implications for optics and remote sensing of natural waters. The upward radiance emerging from the water suffers a critical change when it passes through the water-air interface. Upwelling radiance transmittance $\tau_{w,a}$ is an optical process occurring at the water-air interface that determines the in-water radiances propagating through the interface. In previous studies, $\tau_{w,a}$ was successfully derived for determining the water-leaving radiances in open ocean waters, despite being oversimplified with a constant value. The constant $\tau_{w,a}$ value becomes rapidly invalid in high scattering and absorbing waters within nearshore and inland environments. In this study, we attempt to quantitatively solve the upwelling radiance transmittance $\tau_{w,a}$ (i.e., the percentage of in-water photons that escape through the water-air interface) for varying coefficients of scattering and absorption within the range of natural waters. The two important optical phenomena which are ignored in the previous studies have been fully accounted: (*i*) the particulate contribution to the refractive index (RI) of seawater and (*ii*) the multiple interactions of the upwelling photons with the water-air interface. As a result, this study leads to a new theoretical formulation of the upwelling radiance transmittance applicable to all natural waters. The effect and variation of the new formulation on the water-leaving radiance and remote sensing reflectance is further studied for coastal and inland waters. Particular attention is also focused on the conversion of sub-surface remote sensing reflectance ($r_{rs}$) to above-surface remote sensing reflectance ($R_{rs}$), which is important for calibration and validation of the remote sensing algorithms. The results show substantial improvement in the ocean color quantities ($L_w$ and $R_{rs}$) by up to factor 33% for scattering waters and <5% for absorbing waters.



**OCIS codes:** (010.4450) Oceanic optics; (010.4455) Oceanic propagation; (010.5620) Radiative transfer; (010.5630) Radiometry; (010.7340) Water.

## References and links

1. T. Dickey, M. Lewis, and G. Chang, "Optical oceanography: Recent advances and future directions using global remote sensing and in situ observations," Rev. Geophys. **44**, RG1001 (2006).
2. J. Jaffe, K. Moore, J. McLean, and M. Strand, "Underwater Optical Imaging: Status and Prospects," Oceanography (Wash. D.C.) **14**, 64–75 (2001).
3. J. E. Tyler, *Radiance Distribution as a Function of Depth in the Submarine Environment* (University of California, 1960).
4. J. T. O. Kirk, "The upwelling light stream in natural waters," Limnol. Oceanogr. **34**, 1410–1425 (1989).
5. H. R. Gordon and A. Y. Morel, *Remote Assessment of Ocean Color for Interpretation of Satellite Visible Imagery: A Review* (Springer-Verlag New York Inc., 1983).
6. B. Sundarabalan, P. Shanmugam, and S. Manjusha, "Radiative transfer modeling of upwelling light field in coastal waters," J. Quant. Spectrosc. Radiat. Transf. **121**, 30–44 (2013).
7. A. Gershun, "The light field," J. Math. Phys. **18**, 141–146 (1939).
8. R. W. Preisendorfer, *Radiative Transfer on Discrete Spaces* (Elsevier, 1965).
9. C. L. Wyatt, *Radiometric Calibration: Theory and Methods* (Academic, 1978).
10. C. D. Mobley, "Radiative Transfer: Across the surface," in *Light and Water: Radiative Transfer in the Natural Waters* (Academic, 1994).
11. F. E. Nicodemus, "Radiance," Am. J. Phys. **31**, 368–377 (1963).

#302801 https://doi.org/10.1364/OE.25.027086
Journal © 2017 Received 21 Jul 2017; revised 8 Oct 2017; accepted 8 Oct 2017; published 20 Oct 2017

12. J. Dera, "Marine Physics," in *Elsevier Oceanography Series* (Elsevier, 1992), Vol. 53.
13. R. W. Austin, "Inherent spectral radiance signatures of the ocean surface," in *Ocean Color Analysis* (Scripps Inst. Oceanogr., 1974), p. 2.1–2.20.
14. P. J. Dev and P. Shanmugam, "A new theory and its application to remove the effect of surface-reflected light in above-surface radiance data from clear and turbid waters," J. Quant. Spectrosc. Radiat. Transf. **142**, 75–92 (2014).
15. C. D. Mobley, "Estimation of the remote-sensing reflectance from above-surface measurements," Appl. Opt. **38**(36), 7442–7455 (1999).
16. M. L. Boas, *Mathematical Methods in the Physical Sciences* (Wiley India, 2006).
17. A. Morel and B. Gentili, "Diffuse reflectance of oceanic waters. III. Implication of bidirectionality for the remote-sensing problem," Appl. Opt. **35**(24), 4850–4862 (1996).
18. J. L. Mueller, A. Morel, R. Frouin, C. Davis, R. Arnone, K. Carder, R. G. Steward, S. Hooker, C. D. Mobley, S. Mclean, M. Miller, B. Holben, C. Pietras, G. S. Fargion, K. D. Knobelspiesse, J. Porter, and K. J. Voss, *Ocean Optics Protocols For Satellite Ocean Color Sensor Validation, Revision 4, Volume III : Radiometric Measurements and Data Analysis Protocols. NASA/TM-2003–21621* (2003), Vol. III.
19. A. Morel and B. Gentili, "Diffuse reflectance of oceanic waters. II Bidirectional aspects," Appl. Opt. **32**(33), 6864–6879 (1993).
20. E. Aas, "Refractive index of phytoplankton derived from its metabolite composition," J. Plankton Res. **18**, 2223–2249 (1996).
21. D. Stramski, A. Morel, and A. Bricaud, "Modeling the light attenuation and scattering by spherical phytoplanktonic cells: a retrieval of the bulk refractive index," Appl. Opt. **27**(19), 3954–3956 (1988).
22. H. J. Nasiha, P. Shanmugam, and V. G. Hariharasudhan, "A New Inversion Model to Estimate Bulk Refractive Index of Particles in Coastal Oceanic Waters: Implications for Remote Sensing," IEEE J. Sel. Top. Appl. Earth Obs. Remote Sens. **7**, 3069–3083 (2014).
23. M. S. Twardowski, E. Boss, J. B. Macdonald, W. S. Pegau, A. H. Barnard, and J. R. V. Zaneveld, "A model for estimating bulk refractive index from the optical backscattering ratio and the implications for understanding particle composition in case I and case II waters," J. Geophys. Res. **106**, 14129 (2001).
24. J. R. V. Zaneveld and H. Pak, "Method for the determination of the index of refraction of particles suspended in the ocean*," J. Opt. Soc. Am. **63**, 321 (1973).
25. R. W. Austin and G. Halikas, *The Index of Refraction of Seawater* (University of California at San Diego, 1976).
26. J. L. Mueller and R. W. Austin, *Ocean Optics Protocols for SeaWiFS Validation, Revision 1, Volume 25* (1995).
27. S. K. Sahu and P. Shanmugam, "Semi-analytical modeling and parameterization of particulates-in-water phase function for forward angles," Opt. Express **23**(17), 22291–22307 (2015).
28. R. W. Austin, "Gulf of Mexico, Ocean-color surface-truth measurements," Boundary-Layer Meteorol. **18**, 269–285 (1980).
29. H. R. Gordon, "Dependence of the diffuse reflectance of natural waters on the sun angle," Limnol. Oceanogr. **34**, 1484–1489 (1989).
30. C. S. Roesler, "Theoretical and experimental approaches to improve the accuracy of particulate absorption coefficients derived from the quantitative filter technique," Limnol. Oceanogr. **43**, 1649–1660 (1998).
31. K. Voss and A. Chapin, "Upwelling radiance distribution camera system, NURADS," Opt. Express **13**(11), 4250–4262 (2005).
32. H. R. Gordon and D. K. Clark, "Clear water radiances for atmospheric correction of coastal zone color scanner imagery," Appl. Opt. **20**(24), 4175–4180 (1981).
33. J. Wei, Z. Lee, M. Lewis, N. Pahlevan, M. Ondrusek, and R. Armstrong, "Radiance transmittance measured at the ocean surface," Opt. Express **23**(9), 11826–11837 (2015).
34. Z. Lee, K. L. Carder, C. D. Mobley, R. G. Steward, and J. S. Patch, "Hyperspectral remote sensing for shallow waters. I. A semianalytical model," Appl. Opt. **37**(27), 6329–6338 (1998).
35. H. R. Gordon, J. W. Brown, O. B. Brown, R. H. Evans, R. C. Smith, K. S. Baker, and D. K. Clark, "A semianalytic radiance model of ocean color," J. Geophys. Res. **93**, 10909–10924 (1988).
36. E. Boss, M. S. Twardowski, and S. Herring, "Shape of the particulate beam attenuation spectrum and its inversion to obtain the shape of the particulate size distribution," Appl. Opt. **40**(27), 4885–4893 (2001).
37. C. S. Roesler and E. Boss, "Spectral beam attenuation coefficient retrieved from ocean color inversion," Geophys. Res. Lett. **30**, 1468 (2003).
38. C. D. Mobley, L. K. Sundman, and E. Boss, "Phase function effects on oceanic light fields," Appl. Opt. **41**(6), 1035–1050 (2002).

## 1. Introduction

Spectral radiance ($L$) is the fundamental radiometric quantity used to describe the radiance field of any medium. It is defined as the radiant power ($\Phi$) in a specified direction ($\theta$, $\varphi$) per unit area ($A$), per unit solid angle ($\Omega$), within a wavelength interval ($\Delta\lambda$), and it is expressed in the units of $Wm^{-2}sr^{-1}nm^{-1}$.

$$L(\theta,\varphi,\lambda)=\frac{\Delta^3\Phi}{\Delta A\Delta\Omega\Delta\lambda}. \quad (1)$$

where $\theta$ and $\varphi$ are the viewing and azimuth angles of measurement. In marine optics, the radiances emerging from the ocean provide the knowledge about the light interaction with the seawater and its constituents. The measured optical properties obtained from these interactions have important implications in the other fields of oceanography, such as estimation of heat budget, carbon cycle, upper ocean dynamics, biogeochemistry, underwater visibility studies, and underwater imaging [1,2]. The geometrical structure of the upward radiances in the upper ocean is primarily dependent on the radiance distribution (of downwelling light) above the sea surface [3,4] and secondarily on the inherent optical properties (IOPs) of the seawater. These radiances originate due to the upward scattering events within few optical distances below the sea surface. The upward radiances serve as an optical storehouse of information about the water medium. The remote sensing satellite sensor or a field radiometer placed above the sea surface capture only these upwelling radiances that are transmitted through the water surface [5,6].

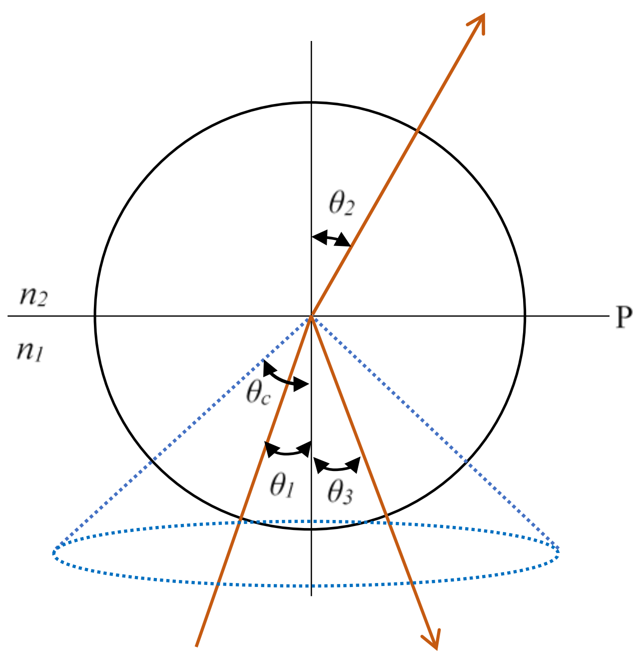


Fig. 1. Systematic geometrical representation of the transfer of radiance from one medium to another $n_1$ and $n_2$ respectively. P is the layer of separation (interface) between the two media, $\theta_1$, $\theta_2$ and $\theta_3$ are the incident, refracted and reflected angles with respect to normal, and $\theta_c$ is the critical angle.

When the radiant flux travels from one medium to the other (air to water or water to air), it undergoes important optical changes at the interface (a layer of separation between the two medium) determined by the *radiance transmission coefficient* or the *radiance transmittance*. Transmission of the radiance across the two-medium interface was first geometrically described by Straubel, known as the *$n^2$ - law for radiances* [7–10] which is one of the most significant laws of geometric optics. For further details on the law and the geometry, refer to Appendix A and Fig. 1. This law has been modified for application to the air-sea interface (also, sea-air) by incorporating the loss of radiance through Fresnel reflection [10–13]. The fully emerged radiance from the water after crossing the water-air interface is known as the water-leaving radiance. Thus, the upwelling radiance after transmission through the water-air interface is given by,

$$L_w\left(air,\lambda\right)=\tau_{w,a}\left(\lambda\right)L_u\left(0^-,\lambda\right). \tag{2}$$

where,

$$\tau_{w,a}\left(\lambda\right)=\frac{t\left(\lambda\right)}{n^2\left(\lambda\right)}=\frac{1-\rho_{w,a}\left(\lambda,\theta_v\right)}{n^2\left(\lambda\right)}. \tag{3}$$

where, $L_u(0^-, \lambda)$ is the upwelling radiance measured at nadir direction just beneath the water surface and $0^-$ represents the point at null depth and $\lambda$ the wavelength. $\tau_{w,a}$ is the *upwelling* radiance transmittance, with the subscript *w,a* denoting the direction of the radiance from water to air, $\theta_v$ represents the viewing angle of the sensor, and $n$ is the refractive index of the seawater. The value of $\tau_{w,a}$ is generally assumed to be 0.541 [14,15], for any Fresnel reflectances ($\rho_{w,a}$) at the water-air interface, ranging between 0.01 to 0.05 for viewing angles less than 40 degrees [13], for the pure seawater with a refractive index (RI) of 1.34.

The form of *upwelling radiance transmittance* [Eq. (3)] derived from the *$n^2$ - law for radiance* exhibits only the *geometrical* behaviour of radiance transmitted from water to air. Although it is theoretically correct based on its geometrical radiometry [Fig. 1], additional contributions of the water medium to $\tau_{w,a}$ are ignored. Our interest is to quantify these contributions to the upwelling radiance transmittance in natural waters, because of the necessity to determine accurate water-leaving radiances emerging from the water body.

This paper attempts to theoretically improve $\tau_{w,a}$ with two other additional contributions which have been ignored in the previous studies. First, the phenomenon of multiple interactions of the radiance with the water-air interface is incorporated into the existing *geometrical upwelling radiance transmittance* through the two important parameters namely, the single scattering albedo ($\omega$) and the upwelling average cosines ($\mu_u$). Second, appropriate refractive index values of seawater are determined that replace the conventional use of pure-water refractive index values based on the particulate contribution to the pure seawater. Using the new theoretical formulation obtained from this study, a conversion of sub-surface $r_{rs}$ to above-surface $R_{rs}$ is achieved. Finally, the significant improvement on the ocean color quantities $L_w$ and $R_{rs}$ is demonstrated using in situ data for the entire bio-optical range of natural waters ($\omega$ = 0 to 0.97).

## 2. Theoretical considerations

The geometrical radiometry provides the radiance transmittance only for the ideal case of zero scattering and zero absorption and the multiple interactions of photons within the interface is completely ignored. Optically, the interface is not just a layer of separation between the two media, but many water constituents present within this layer play a crucial role in determining the transmission of radiances through it. The radiance transfer process from water to air is very complex because the water medium (originating side) is denser than the air and is composed of many particles. In this section, factors affecting the *upwelling radiance transmittance* $\tau_{w,a}$ is addressed based on some theoretical considerations of the water-air interface optical processes.

### *2.1. Multiple interactions of radiances at the water-air interface*

The transfer of upwelling radiance through the water-air interface predominantly relies on the geometrical radiometry, which is however insufficient to explain the interface optical processes considering the fact that multiple interactions of photons occur at the water-air interface and many particles are included in it. Here, two cases are presented: (i) a hypothetical case by assuming the water medium as a non-absorbing medium (i.e., fully scattering), and (ii) a realistic case of natural waters.

### 2.1.1. For non-absorbing media

Let us designate $\tau_{pw,a}$ as the *pure water geometrical upwelling radiance transmittance*, the value is simply 0.541 and $\tau_{w,a}$ is the newly derived *upwelling radiance transmittance* incorporating the multiple interactions of the photons with the water-air interface. The assumption of 0.541 as the transmission factor [Eq. (2)], states that 54.1% of in-water photons escape through the water-air interface leaving the rest of the photons (i.e 45.9%) within the water medium itself. On the first interaction of a photon with the water-air interface, according to the law of conservation of energy, $(1-\tau_{pw,a})$ is retained within the water column. If there is no absorption within the water-air interface, and if all photons are directed back to the interface again through the upward scattering by the particles (this assumption does not hold naturally), then, the $(1-\tau_{pw,a})$ photons take a second attempt ($i = 2$) to cross the interface. Here, $i$ denotes the number of interactions of a single photon with the water-air interface. On the second successive interaction ($i = 2$), based on the geometry, $\tau_{pw,a}$ part of $(1-\tau_{pw,a})$ is allowed to cross the interface. As a result, $\tau_{pw,a}(1-\tau_{pw,a})$ escapes through the interface giving the value of 0.248. For every successive interaction of the photon with the interface, the geometry appears the same and considers it as an new photon entering the interface. At the end of the second successive interaction $[\tau_{pw,a} + \tau_{pw,a}(1-\tau_{pw,a})]$, 78.9% of photons have crossed the interface. Similarly, on the third successive interaction ($i = 3$), $\tau_{pw,a}(1-\tau_{pw,a})^2$ escapes the interface producing 90.3% $[\tau_{pw,a} + \tau_{pw,a}(1-\tau_{pw,a}) + \tau_{pw,a}(1-\tau_{pw,a})^2]$ of photons escaping the interface. Finally, for a complete transfer of photons from the water medium to air, it would take at least ten interactions (Table 1) given only if the water medium is totally non-absorbant and all the photons are redirected to the surface.

**Table 1. Successive interactions of the photons escaping the water-air interface for a non-absorbing medium.**

| Successive interaction of photons escaping the water-air interface | Value ($\tau_{w,a}$) | Successive addition (*non-absorbing medium*) |
|---|---|---|
| $[i = 1]\ \tau_{pw,a}$ | 0.541 | 0.541 $[\tau_{pw,a}]$ |
| $[i = 2]\ \tau_{pw,a}(1-\tau_{pw,a})$ | 0.248 | 0.789 $[\tau_{pw,a} + \tau_{pw,a}(1-\tau_{pw,a})]$ |
| $[i = 3]\ \tau_{pw,a}(1-\tau_{pw,a})^2$ | 0.114 | 0.903 $[\tau_{pw,a} + \tau_{pw,a}(1-\tau_{pw,a}) + \tau_{pw,a}(1-\tau_{pw,a})^2]$ |
| $[i = 4]\ \tau_{pw,a}(1-\tau_{pw,a})^3$ | 0.052 | 0.956 $[\tau_{pw,a} + \tau_{pw,a}(1-\tau_{pw,a}) + \ldots\ldots\ldots + \tau_{pw,a}(1-\tau_{pw,a})^3]$ |
| $[i = 5]\ \tau_{pw,a}(1-\tau_{pw,a})^4$ | 0.024 | 0.980 $[\tau_{pw,a} + \tau_{pw,a}(1-\tau_{pw,a}) + \ldots\ldots\ldots + \tau_{pw,a}(1-\tau_{pw,a})^4]$ |
| $[i = 6]\ \tau_{pw,a}(1-\tau_{pw,a})^5$ | 0.011 | 0.991 $[\tau_{pw,a} + \tau_{pw,a}(1-\tau_{pw,a}) + \ldots\ldots\ldots + \tau_{pw,a}(1-\tau_{pw,a})^5]$ |
| $[i = 7]\ \tau_{pw,a}(1-\tau_{pw,a})^6$ | 0.005 | 0.996 $[\tau_{pw,a} + \tau_{pw,a}(1-\tau_{pw,a}) + \ldots\ldots\ldots + \tau_{pw,a}(1-\tau_{pw,a})^6]$ |
| : | : | : |
| $[i = 10]\ \tau_{pw,a}(1-\tau_{pw,a})^9$ | 0.000 | 1.000 $[\tau_{pw,a} + \tau_{pw,a}(1-\tau_{pw,a}) + \ldots\ldots\ldots + \tau_{pw,a}(1-\tau_{pw,a})^9]$ |

On the assumption of above conditions and inclusion of multiple interactions of the photons with the water-air interface on the existing geometry for pure water, the upwelling radiance transmittance is theoretically derived as follows:

$$\begin{aligned}\tau_{w,a} &= \tau_{pw,a} + \tau_{pw,a}\left(1-\tau_{pw,a}\right) + \tau_{pw,a}\left(1-\tau_{pw,a}\right)^2 + \tau_{pw,a}\left(1-\tau_{pw,a}\right)^3 + \ldots. \\ &= \tau_{pw,a}\left\{1 + \left(1-\tau_{pw,a}\right) + \left(1-\tau_{pw,a}\right)^2 + \left(1-\tau_{pw,a}\right)^3 + \ldots\right\}.\end{aligned} \tag{4}$$

On solving, Maclaurin series is deduced as a part, and is replaced by $(\tau_{pw,a})^{-1}$ [16].

Optics EXPRESS

$$= \tau_{pw,a} \left\{ \frac{1}{\tau_{pw,a}} \right\}. \qquad (5)$$

$$\tau_{w,a} = 1.$$

Equation (5) gives the upwelling radiance transmittance for the non-absorbing medium, which is equivalent to one, which means all photons escape through the interface.

According to the law of conservation of energy, for a non-absorbing medium, the maximum value that can be attained is 1. As expected, the new radiance transmittance $\tau_{w,a}$ gives the value of 1. The percentage of photons escaping the interface on each event is comprehensively described in Table. 1, which suggests that the maximum number of interactions can go up to ten ($i$ = 10). Geometrically, on every possible interaction, 54.1% of the photons escapes the interface. Accordingly, on the first interaction ($i$ = *1*), 54.1% escapes the interface, 78.9% on the second ($i$ = *2*), 90.3% on the third ($i$ = *3*), 95.6% on the fourth ($i$ = *4*), and 98.0% on the fifth ($i$ = *5*), and so on. Note that at the tenth interaction, 100% of the photons would have crossed the interface, and consequently, no more photons are there to undergo for the next interaction to any further extent. From this theory, it can be concluded that there is no more interaction of the upward photons with the water-air interface beyond $i$ = 10 as the number of interactions is always quantized.

### 2.1.2. For the case of natural waters

The previous section on describing the upwelling radiance transmittance for a non-absorbing medium gives a clear picture to understand the optical processes occurring at the interface. Nonetheless, the assumption made for the non-absorbing case is no longer justified for the case of natural waters. Unlike the non-absorbing case, the photons are subject to get absorbed and scattered depending upon the types of particles (and dissolved substances) present in natural waters. This means that the photons are restricted to further interact with the interface for the successive times. To address the complete multiple interactions of the photons along with the water scattering and absorption processes within the interface, the optical processes must be stated clearly. First, it is essential to have knowledge of how many photons actually survive after a collision with the water molecules and particles. As the water molecules and particles continue to absorb and scatter the photons incident on them, the number of escaping photons depends on the survival index. The survival index is an IOP (inherent optical property) which can be termed as the *probability of photon survival* or the *single scattering albedo* $(\omega = b / c)$. The *probability of a photon survival* describes the fraction of photon scattering '*b*' over the extinction '*c*' which gives the percentile estimate of the survival photons after every collision or interaction. The survival index is low for an absorbing medium and high for a scattering medium. In other terms, the survival index of a photon describes the probability of the photon that is scattered rather than absorbed. In an absorbing medium, only less number of photons are gone for further interaction with the interface, whereas in a scattering medium more number of photons are involved. Second, not all survived photons (which are scattered in all directions) travel upward to escape through the interface. Therefore, the probability of upward scattered photons should be estimated in order to determine the proportion of upwelling photons. The proportion of upward photons depends on the angular distribution of the upward scattered flux known as upwelling average cosines, $\mu_u$.

The single scattering albedo multiplied with the average upwelling cosine (i.e., $\mu_u \omega$) completely describes the percentage of upwelling photons emerging from the water medium after interaction with a water molecule or a particle. The $\mu_u \omega$ plays a role whenever the photon is available for the next successive interactions, therefore, it is multiplied by the successive geometrical upwelling radiance transmittances ($\tau_{pw,a}$). The radiance transmittance ($\tau_{w,a}$) for '$i$' number of interactions with the interface and the molecule/particle is given by

$$\begin{aligned}\tau_{w,a} &= \tau_{pw,a} + \mu_u\omega\tau_{pw,a}\left(1-\tau_{pw,a}\right) + \mu_u\omega\tau_{pw,a}\left(1-\tau_{pw,a}\right)^2 + \mu_u\omega\tau_{pw,a}\left(1-\tau_{pw,a}\right)^3 + \ldots \\ &= \tau_{pw,a} + \mu_u\omega\tau_{pw,a}\left(1-\tau_{pw,a}\right)\left\{1+\left(1-\tau_{pw,a}\right)+\left(1-\tau_{pw,a}\right)^2+\left(1-\tau_{pw,a}\right)^3+\ldots\right\}.\end{aligned} \tag{6}$$

On solving, Maclaurin series is deduced as a part, and is replaced by $(\tau_{pw,a})^{-1}$ [16].

$$\begin{aligned} &= \tau_{pw,a} + \mu_u\omega\tau_{pw,a}\left(1-\tau_{pw,a}\right)\times\left\{\frac{1}{\tau_{pw,a}}\right\}. \\ &= \tau_{pw,a} + \mu_u\omega\left(1-\tau_{pw,a}\right). \\ \tau_{w,a} &= \tau_{pw,a}\left(1-\mu_u\omega\right)+\mu_u\omega. \end{aligned} \tag{7}$$

From Eq. (7), it is explicit that the minimum transmittance depends on the geometrical radiometry and additional contribution is due to multiple interactions of the photons with the interface.

### 2.2. Particulate contribution to the refractive index of seawater

The refractive index of seawater ($n$) is bound together with the $n^2$ - *law for radiance* that corresponds to the geometrical part of the radiance transmittance. However, the notation '$n$' collectively represents the refractive index of the particulate matter and the pure seawater. In practice, the refractive index of pure seawater [particularly in Eq. (3)] is generally assumed for most oceanic applications [13,17–19]. Since the constant pure water refractive index value only partially accounts for the water-air interface optical process, it is not suitable for applications in the nearshore and inland environments with significant particulate loads [20–24]. Thus, determination of the particulate refractive index is necessary and it is generally deduced relative to pure seawater [23,24]. In this context, the refractive index of seawater is defined as the product of RI of pure seawater $n_w(\lambda)$ and RI of particulate matter relative to pure seawater $r_f$, which is expressed as a wavelength-dependent form

$$n(\lambda) = n_w(\lambda)\times r_f. \tag{8}$$

where, $n_w(\lambda)$ is the wavelength-dependent refractive index of seawater which is empirically formulated from the data of Austin and Halikas (1976) [25,26] and given in Eq. (9).

$$n_w(\lambda) = 1.325147 + \frac{6.6096}{\lambda - 137.1924}. \tag{9}$$

Particulate refractive index $r_f$ can be calculated from the model of Sahu and Shanmugam [27] specified in Appendix B.

## 3. Theoretical radiance transmittance for natural waters

The theoretically deduced Eq. (7) successfully replaces the conventional *pure water geometrical upwelling radiance transmittance* with the '*actual*' *upwelling radiance transmittance*. Combining Eqs. (7) and (8), we obtain,

$$\tau_{w,a} = \left(\frac{\left(1-\rho_{w,a}\right)}{n_w^2}\times\frac{(1-\mu_u\omega)}{r_f^2}\right)+\mu_u\omega.$$

Rearranging, we get

$$\tau_{w,a} = \frac{(1-\rho_{w,a})}{n_w^2}\left[\frac{(1-\mu_u\omega)}{r_f^2} + \frac{\mu_u\omega n_w^2}{(1-\rho_{w,a})}\right]. \tag{10}$$

Substituting Eq. (10) in Eq. (2), we get the actual water-leaving radiances from

$$L_w(air,\lambda) = \frac{(1-\rho_{w,a})}{n_w^2}\left[\frac{(1-\mu_u\omega)}{r_f^2} + \frac{\mu_u\omega n_w^2}{(1-\rho_{w,a})}\right] L_u(0^-,\lambda). \tag{11}$$

Here, the wavelength symbols ($\lambda$) are omitted for brevity. The $\rho_{w,a}$ on in-water radiometry was experimentally studied by Austin for various wind speed conditions [13]. The time-averaged water-air Fresnel reflectance observations showed the effects and influences of wind speed which is substantially weak regardless of the sea-state conditions [15,28].

## 4. Results and discussion

From the new theory, it is intuitively understood that the radiance transmittance is not a constant value, but it is strongly dependent on the geometry and multiple interactions of the radiance with the water-air interface. The existing *geometrical upwelling radiance transmittance* equation $(1-\rho_{w,a})/n_w^2$ partially accounts for the refractive index of natural water (since it considers the pure water RI), and hence, its application is restricted to open ocean waters. The new radiance transmittance formulation is derived theoretically by incorporating the additional influences due to the refractive index of particles and the multiple interactions of the photons with the interface. Thus, the new formulation of radiance transmittance [Eq. (10)] is applicable for most natural waters.

### *4.1 Water-air interface and the upward radiances*

To determine the water-leaving radiance $L_w(air,\lambda)$ from the upwelling radiance $L_u(0^-,\lambda)$, accurate quantification of $\tau_{w,a}$ is necessary. This requires a better understanding of the behaviour of upward scattered photons emerging from the water. Upward travelling photons have the greater probability of escaping the interface unless they are redirected back to the water medium by the Fresnel reflection on the water side and the downward scattering by the water molecules and particles. The upward radiance is dependent on the incoming solar (downwelling) flux penetrating into the water and is the result of upward scattering by the molecules and the particles present in it. A collection of upward scattered photons within a solid angle is known as the radiance obeys $(1-\rho_{w,a})/n_w^2$ law and crosses the interface, while the rest of the photons are redirected back to the water medium. The redirected photons are presumably diverted to any direction within the lower hemisphere of the water surface, and sometimes depend on the sea state. It should be pointed out that the directionality of the photon may depend on the sea-state [29], but the $(1-\rho_{w,a})$ remains unaffected [28]. The redirected photons from the interface cannot freely travel along the direction to which it was focussed, but have interactions with all the particles and water molecules along its path and get modified by the absorption and scattering processes. Few parts of photon energy are lost by absorption and the rest are scattered into other directions according to the shape of the volume scattering function. However, the probability for a (redirected) photon that is scattered upward depends upon two factors – *single scattering albedo* '$\omega$' and *upwelling average cosine* '$\mu_u$'. The single scattering albedo $\omega(=b/c)$ provides the probability for a photon being scattered rather than absorbed, and has the ability to describe the type of the particle but not the scattered direction. For the scattering direction to be known after single scattering, the average cosine of the light field '$\mu$' provides a better estimate of the photon direction. As our interest lies in the photon that is scattered upward, the upwelling average cosine for the upward light field $\mu_u$ gives the probability of photon direction. The upwelling light field originates from upward scattering events at lower depths, which is completely diffuse and can be assumed to be isotropic. Therefore, the average cosine for the upwelling light field is considered as 0.5 [30,31].

$$\mu_u = \overline{\cos\theta} = \frac{\int_0^{\pi}\cos\theta d\omega}{\int_0^{\pi} d\omega} = 0.5. \tag{12}$$

where, $d\omega = \sin\theta d\theta d\phi$ , and $\theta$ is the direction of the scattered photon.

Comprehensively, the probability of a scattered photon is signified by $\omega$ and $\mu_u\omega$ is the probability of the upward scattered photon. The new terms $(1-\mu_u\omega)/r_f{}^2$ and $\mu_u\omega n_w^2/(1-\rho_{w,a})$ in Eq. (7) are highly responsible for the multiple interactions of photons with the interface, which allow some extra photons to cross the interface in addition to the $\left(1-\rho_{w,a}\right)/n_w^2$. $\left(1-\rho_{w,a}\right)/n_w^2$ is the *pure water geometrical upwelling radiance transmittance*, a percentile estimate of the photons crossing the interface based on the geometrical radiometry for the pure water condition, and holds the value of 0.541 (or 54.1%). The particulate refractive index $r_f$, however, an inclusive part of the geometry, is described relative to the *pure water geometrical radiance transmittance* $\tau_{w,a}$. The ratio between the 'actual' *radiance transmittance* $\tau_{w,a}$ and the *pure water geometrical radiance transmittance* $\tau_{pw,a}$ is equivalent to $\left(1-\mu_u\omega\right)/r_f^2 + \mu_u\omega n_w^2/(1-\rho_{w,a})$ .

$$\frac{\tau_{w,a}}{\tau_{pw,a}} = \frac{\left(1-\mu_u\omega\right)}{r_f^2} + \frac{\mu_u\omega n_w^2}{(1-\rho_{w,a})}. \tag{13}$$

The particulate refractive index is always greater than or equal to one, *i.e.* $r_f \geq 1$. The increase of particulates in the water decreases the *radiance transmittance* by the square value of $r_f$.

### *4.2 Examination of theoretical upwelling radiance transmittance with in situ data*

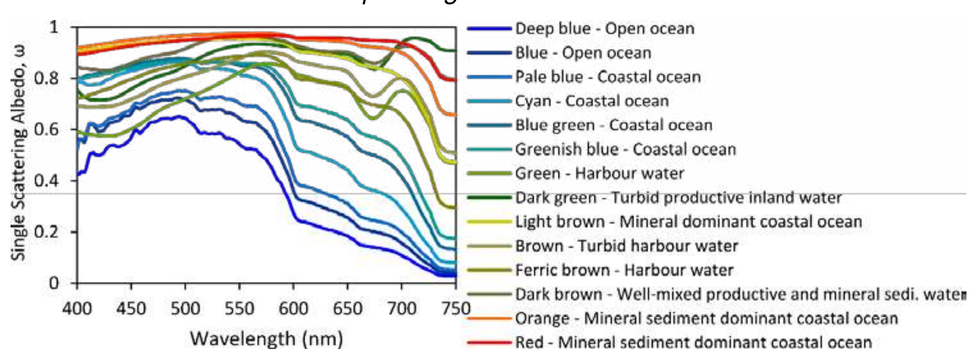


Fig. 2. In situ measured data of single scattering albedo $\omega(=b/c)$ for 14 different environments representing the clear oceanic waters (deep blue) to highly turbid scattering waters (red). This plot clearly shows the effects of absorption and scattering with respect to the wavelength. The lowest and highest values of $\omega$ measured being near zero for clear open oceanic waters (at a wavelength 750 nm) and 0.97 for mineral rich turbid waters (at a wavelength 715 nm).

We now examine the theoretically derived radiance transmittance $\tau_{w,a}$ [Eq. (7)] with the *in situ* data. To examine any improvement and difference between the old and the new transmittance formulations, we intended to select the data from various water bodies which are unique and different from each other in their spectral characteristics. Based on this criterion, fourteen data were selected from different stations in clear oceanic waters of southern Bay of Bengal, relatively clear waters of coastal Chennai (slightly increased turbidity as compared to the clear oceanic waters), sediment-dominated waters off Point Calimere, and turbid productive inland waters of Muttukaadu lagoon. These data are optically different from each other that can be recognized from the spectral plots of $\omega$ [Fig. 2].

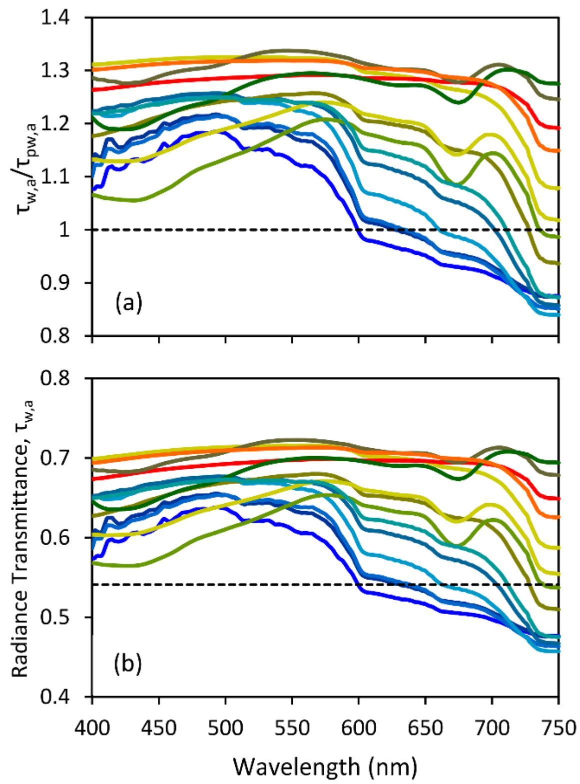


Fig. 3. (a) Plot of the additional term $\left(1-\mu_u\omega\right)/r_f^2+\mu_u\omega n_w^2/(1-\rho_{w,a})$ representing the ratio of new theoretical upwelling radiance transmittance $\tau_{w,a}$ relative to the pure water geometrical upwelling radiance transmittance $\tau_{w,a}$ (The black dots in 'a' represent $\tau_{w,a}$:$\tau_{pw,a}$ = 1). (b) The new theoretical upwelling radiance transmittance $\tau_{w,a}$ is applied for the natural water types with measured $\omega$ values ranging from 0 to 1 (The black dots in 'b' represent $\tau_{pw,a}=(1-\rho_{w,a})/n_w^2\approx 0.541$ line). The legends of these spectra are given in Fig. 2.

The difference between the $\tau_{w,a}$ and $\tau_{pw,a}$ mainly comes from the three independent factors $\mu_u$, $\omega$, and $r_f$. Assuming $\mu_u$ = 0.5, $\omega$ from *b/c* via *in situ* measurements, and $r_f$ from the existing model (shown in Appendix B), the new radiance transmittance $\tau_{w,a}$ is calculated. As $\mu_u$ is assumed as constant, the variation in $\tau_{w,a}$ is due to the $\omega$ and $r_f$ values. The $\omega$ is a spectrally dependent parameter and highly sensitive to the water types. Figure 2 gives the trend of $\omega$ depicting the spectral variations for 14 different water types. $\omega$ is low for clear oceanic waters (around 0.4 in the blue region and nearly zero in the red region), indicating that the scattering probability is relatively high in the blue bands and low in the red bands due to the dominance of water molecules. In contrast, the value of $\omega$ increases with the increasing particulate concentration in other water types, as shown by various colors for clear open ocean waters, coastal waters, CDOM and phytoplankton dominant harbour waters, phytoplankton dominant inland waters and mineral sediment dominant coastal waters. Low values of $\omega$ indicate the tendency of the particles being inclined towards the absorption and high values towards the scattering. Much variations in the magnitude of $\omega$ are noticed at longer wavelengths than shorter wavelengths because of the increased water absorption and particulate scattering. The larger water content in the case of clear oceanic waters causes the water absorption to dominate at longer wavelengths, and the relatively lesser water content in particle-rich coastal and inland waters causes the scattering to dominate the optical processes at these wavelengths. The value of $\omega$ goes very high, nearly close to 1, especially in mineral-rich sediment waters because of the high particulate scattering events.

Most importantly, it is observed that the variation in the spectra of $\omega$ is small for high scattering waters and large for clear oceanic waters. This reveals that the spectral variations in $\omega$ have direct effects on the radiance transmittance $\tau_{w,a}$. For instance, $\omega$ for clear oceanic waters is approximately zero at longer wavelengths, with the particulate refractive index $r_f$ closer to 1, and therefore, $\mu_u\omega$ reaches to zero, resulting the new term $\left(1-\mu_u\omega\right)/r_f^2+\mu_u\omega n_w^2/(1-\rho_{w,a})$ to 1. This shows that typically no photons actually emerge at longer wavelengths in the case of clear oceanic waters, and therefore, $\tau_{w,a}$ is almost equivalent to the *pure water geometrical upwelling radiance transmittance*, $\tau_{pw,a}$. However, in the case of high scattering waters with $\omega$ = 0.95, $\mu_u$ = 0.5 and $r_f$ = 1.1 (for mineral waters [23]), the value of $\mu_u\omega$ is 0.475 resulting the new term to 1.31, and therefore, $\tau_{w,a}$ equals the value of 0.709 which is 1.31 times higher than the $\tau_{pw,a}$. Thus, by the process of multiple interactions of the photons with the interface, more number of photons are expected to escape through the interface.

In short, the additional term $\left(1-\mu_u\omega\right)/r_f^2+\mu_u\omega n_w^2/(1-\rho_{w,a})$ describes the considerable role of particles on the upwelling radiance transmittance. From this it is clearly evident that the multiple interaction of the photons with the interface always enhances the $\tau_{w,a}$ to be greater than 0.541. As evident in Fig. 3(a), the value of $\tau_{w,a}$ also seems to fall below 0.541 (denoted by the dotted line) at some spectral domains that are inclined toward the absorption. The fall of $\tau_{w,a}$ below 0.541 is due to the refractive index of particles '$r_f$' which tend to trap the photon within (its medium) itself. According to our investigation, two types of waters can have the probability of $\tau_{w,a}$ falling below the value 0.541: (i) waters with the relatively larger water content characterized by strong absorption of the water molecules particularly at longer wavelengths, and (ii) waters with dominant phytoplankton and/or CDOM which are inclined toward strong absorption particularly in the shorter wavelengths. The higher $\tau_{w,a}$ values are caused by scattering particles as it can be seen at the longer wavelengths [Fig. 3(b)]. $\tau_{w,a}$ of high scattering waters is nearly constant throughout the spectrum, even reaching beyond 0.72. Interestingly, $\tau_{w,a}$ is also much higher in turbid productive waters (a dark brown color spectrum, with high contents of phytoplankton, detritus, mineral sediments, and CDOM) similar to the purely mineral sediment dominated water. The findings reveal that $r_f$ seems to play a major role in determining the magnitude of $\tau_{w,a}$. While the two mineral dominant stations have the $r_f$ values of 1.139 and 1.151, the turbid productive water station with mixed concentrations of phytoplankton, mineral sediments and detritus is characterized by $r_f$ = 1.07 (see these station spectra located nearby). Since the $r_f$ values of the two mineral dominant water stations (1.139 and 1.151) are greater than the $r_f$ value of the well-mixed turbid productive water station (1.07), the low $r_f$ allows more photons to transmit through the interface and hence the high $\tau_{w,a}$ values for these waters.

### *4.3. Conversion of sub-surface $r_{rs}$ to above-surface $R_{rs}$*

Remote sensing reflectance ($R_{rs}$) is the ratio of water-leaving radiance ($L_w$) to the incoming downwelling irradiances ($E_d(0^+, \lambda)$) measured above the water surface [Eq. (14)]. Similarly, sub-surface reflectance ($r_{rs}$) can be calculated as the ratio of upwelling radiances ($L_u(0^-,\lambda)$) (measured at nadir position) to the downwelling irradiances ($E_d(0^-,\lambda)$) below the water surface [Eq. (15)].

$$R_{rs}\left(0^{+},\lambda\right)=\frac{L_{w}\left(air,\lambda\right)}{E_{d}\left(0^{+},\lambda\right)}. \tag{14}$$

$$r_{rs}\left(0^{-},\lambda\right)=\frac{L_{u}\left(0^{-},\lambda\right)}{E_{d}\left(0^{-},\lambda\right)}. \tag{15}$$

The conversion of sub-surface $r_{rs}$ to above-water $R_{rs}$ can be achieved by taking the simple ratio of Eq. (14) and Eq. (15),

$$\frac{R_{rs}(0^{+},\lambda)}{r_{rs}(0^{-},\lambda)}=\frac{L_{w}(air,\lambda)}{E_{d}(0^{+},\lambda)}\times\frac{E_{d}(0^{-},\lambda)}{L_{u}(0^{-},\lambda)}. \tag{16}$$

The relation between the irradiances above and below the sea surface is given by [32],

$$E_{d}\left(0^{-},\lambda\right)=\left(1-\rho_{a,w}\right)E_{d}\left(0^{+},\lambda\right). \tag{17}$$

Substituting Eq. (11) and (17) in Eq. (16), we get the exact relation between in-water $r_{rs}$ and above-water $R_{rs}$,

$$R_{rs}\left(0^{+},\lambda\right)=\frac{\left(1-\rho_{a,w}\right)\left(1-\rho_{w,a}\right)}{n_{w}^{2}}\left[\frac{\left(1-\mu_{u}\omega\right)}{r_{f}^{2}}+\frac{\mu_{u}\omega n_{w}^{2}}{\left(1-\rho_{w,a}\right)}\right]r_{rs}\left(0^{-},\lambda\right). \tag{18}$$

where $\rho_{a,w}$ and $\rho_{w,a}$ are Fresnel reflectances of the water-air and air-water respectively, and both hold the approximate value of 0.028; $\mu_u$ = 0.5; $r_f$ obtained from Eq. (35) (given in Appendix B); $\omega$ can be obtained from in situ photometric measurements of scattering '$b$' and attenuation '$c$' coefficients. From Eq. (18), the transmittance of a remote sensing signal from sub-surface to above-surface is equivalent to $\tau_{w,a}(1\text{-}\rho_{a,w})$.

$$R_{rs}\left(0^{+},\lambda\right)=\tau_{w,a}\left(1-\rho_{a,w}\right)\times r_{rs}\left(0^{-},\lambda\right). \tag{19}$$

where, $\tau_{w,a}$ is given in Eq. (10).

### *4.4. Improvement in the ocean color quantities, $L_w$ and $R_{rs}$*

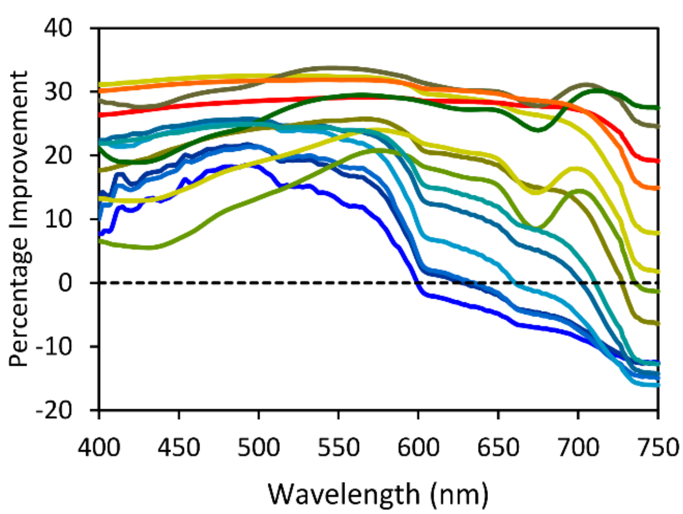


Fig. 4. Spectral relative percentage of improvement in the ocean color quantities, $L_w$ and $R_{rs}$.

Optics EXPRESS

Improvement of the new theoretical formulation [Eq. (10)] over the constant upwelling radiance transmittance ( = 0.541) can be seen by comparing the 0.541 (dotted) line and other spectra in Fig. 3(a)-(b) and the percentage of improvement in Fig. 4. Based on the assessment of the results in Fig. 3(a)-(b), the deviation of the present formulation $\tau_{w,a}$ with the globally considered constant value 0.541 is minimum for the waters characterized by the weak scattering components (CDOM and phytoplankton dominant) and maximum for the waters characterized by the strong scattering components (mineral-rich sediment dominated waters). Any improvement in the $\tau_{w,a}$ is consequently reflected on the water-leaving radiance ($L_w$) and remote sensing reflectance ($R_{rs}$) spectra with the same percentage of improvement.

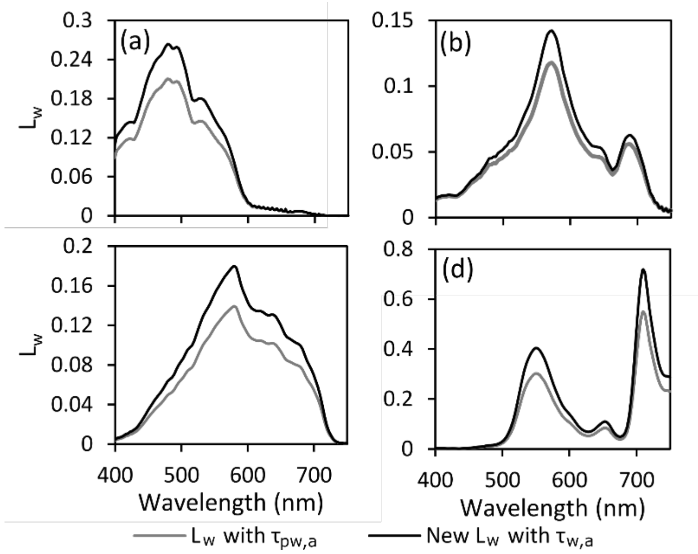


Fig. 5. Water-leaving radiance ($L_w$) determined using the conventional radiance transmittance (grey line) and new theoretical radiance transmittance (dark line) values for four different water types (clear oceanic water – (a), harbour water – (b), turbid coastal water (mineral) – (c), and turbid productive inland water – (d)). Water-leaving radiance ($L_w$) determined using the conventional radiance transmittance (grey line) and new theoretical radiance transmittance (dark line) values for four different water types (clear oceanic water, harbour water, turbid coastal water (mineral), and turbid productive inland water).

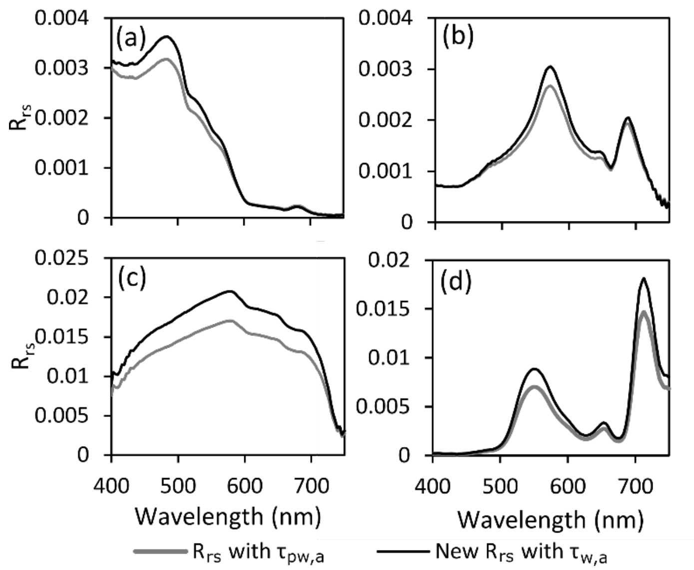


Fig. 6. Remote sensing reflectances ($R_{rs}$) determined using the conventional radiance transmittance (grey line) and new theoretical radiance transmittance (dark line) values for four different water types (clear oceanic water – (a), harbour water – (b), turbid coastal water (mineral) – (c), and turbid productive inland water – (d)).

For oceanic waters (blue to pale green waters), improvement in $L_w$ and $R_{rs}$ spectra is found from 0% to 18% for the wavelength range 400-600nm and goes up to −18% for the wavelength range 600-750 nm, respectively. Here, the (-) minus sign does not denote under performance, but it infers the deviation from the standard value. The harbour waters with high CDOM content and phytoplankton concentration showed up to 22% for the wavelength range 400-750, while the well-mixed turbid productive water with equal parts of phytoplankton and mineral sediments had the range from 20% to 33% for the entire visible wavelengths 400-700nm. The percentage of improvement in high scattering mineral sediment waters varies from 20% to 30% for the entire visible wavelengths. The comparison of the ocean color quantities $L_w$ and $R_{rs}$ determined using the conventional method and the new method Eqs. (11) and (18) is shown in Figs. 5 and 6. The results show significant improvement in the $L_w$ and $R_{rs}$ values.

### *4.5. Comparison of the new theoretical formulation with existing models*

Recently, Wei *et al*. [33] examined the long-standing presumption of constant upwelling radiance transmittance based on their *in situ* measurements of $L_w(air, \lambda)$ and $L_u(0^-,\lambda)$ by adopting the skylight-blocked approach. They studied the relative percentage difference of the transmittance $(= L_w(air,\lambda)/L_u(0^-,\lambda))$ and the constant 0.54 for the three different water types of blue, turquoise blue and green color. Their $\tau_{w,a}$ for the blue waters showed the minimum value of 0.4 and maximum value of 0.6 and the mean percentage difference approximately 5% for the 350-600 nm range and ± 20% for the 600-700 nm range. The conclusion of their results that yielded −20% in the red bands for blue waters is mainly due to the discrepancies and errors. According to our observations on their data, the −20% difference in the red bands is acceptable as only few photons are expected to cross the interface due to the strong absorption by water molecules. Therefore, such a high difference is possible (not mainly due to errors) and it is consistent with the present study. As expected, the turquoise blue and green waters showed less deviations (within 6%), whereas our results are in agreement with the difference of 0-10% for similar water types.

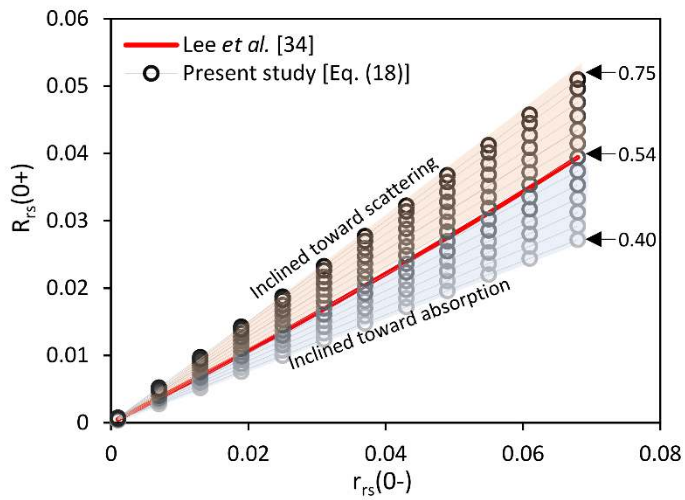


Fig. 7. Comparison of the conversion of sub-surface remote sensing reflectance, $r_{rs}(0^{-},\lambda)$, to above-surface remote sensing reflectance, $R_{rs}(0^{+},\lambda)$, using the present formulation [Eq. (18)] (derived as a function of $\omega$ and $r_f$) and the model of Lee *et al*. [34] (shown in red line). The lowest line represents the transmission factor for a sub-surface remote sensing signal, $\tau_{w,a}(1-\rho_{a,w}) = 0.40$, and the highest line represents the $\tau_{w,a}(1-\rho_{a,w}) = 0.75$. The blue and orange shaded regions depict the waters inclined toward absorption and scattering respectively.

Lee *et al*. [34] presented the relation between $R_{rs}$ and $r_{rs}$ with the constant coefficients [Eq. (24) and (25)], a semi-analytically modified version of Gordon & Clarke and Gordon *et al*. [32,35]. The term $(1-\rho_{a,w})(1-\rho_{w,a})/n_w^2$ of the present study and ζ of Lee *et al.* [34] are analogous to each other and gives the value of 0.518 with the assumed spectrally constant $n_w$ value. However, the difference arises from the next term $\left(1-\mu_u\omega\right)/r_f^2+\mu_u\omega n_w^2/(1-\rho_{w,a})$ and $1/(1-\Gamma r_{rs})$ in which the former term describes the contribution of particulate RI and the multiple interactions of the photons with the interface from the water side and the latter term presents some generalized effects of internal reflection from water to air.

According to Eq. (19), the transmission coefficient for a sub-surface remote sensing signal is $\tau_{w,a}(1-\rho_{a,w})$. $\tau_{w,a}(1-\rho_{a,w})$ for the previous models are approximately closer to 0.54, whereas the present study gives 0 to 0.75 for varying $\omega$ and $r_f$ values. Figure 7 shows the approximate range of variations in the transmittance for a sub-surface remote sensing signal of Lee *et al.* [34] and the present study [Eq. (18)]. The model of Lee *et al.* [34] provides almost constant transmittance, $\tau_{w,a}(1-\rho_{a,w})$~0.54, as shown in red line, whereas the present study provides a wide range of $\tau_{w,a}(1-\rho_{a,w})$ values from 0.40 to 0.75. The values below the red line correspond to the waters inclined toward absorption (blue shaded region) and the values above the red line are inclined toward the scattering (orange shaded region). Comparing both the formulations, the new theoretical formulation successfully takes into account the two key optical processes occurring within the interface for predicting a wide range of transmittance values for natural waters, which enable more accurate remote sensing reflectances for various water color applications.

## 5. Summary and conclusion

The present work replaces the standard upwelling radiance transmittance with the new theoretical upwelling radiance transmittance formulation with potential applications in all natural waters. This new expression serves the purpose of translating the in-water radiance to above surface radiance through the water-air interface, accounting all optical variations from low to high scattering and low to high absorbing waters. The new formulation is exact, in which the geometric conditions and optical phenomenon occurring at the water-air interface including the multiple interactions of photons and the particle optical properties are acknowledged. The results show that the inclusion of new parameters to the geometrical radiance transmittance has led to significant improvement in the accuracy of the determination of the water-leaving radiances and remote sensing reflectances from the below-water radiance measurements (significantly from 0 to 33% depending upon the water types). The percentage improvement is high for the scattering waters and low for the absorbing waters. This study will be important for accurately determining the upwelling radiances that cross the water-air interface in marine and inland environments, where the former approaches are inadequate considering the different types of waters. The new theoretical method will have direct implications for improving the radiometric water color measurements and calibration and validation of space-borne ocean color sensors.

## Appendix A: *$n^2$ - law for radiance*

The $n^2$ - *law for radiance* is an important law of geometrical radiometry which describes the transfer of light rays from one medium to another medium. Let us assume a ray of light incident on the plane P with the angle $\theta_1$ in the medium $n_1$ and refracted with the angle $\theta_2$ in the medium $n_2$ [Fig. 1]. We use the suffixes 1 and 2 to denote the incident and refracted mediums, respectively. According to the *Snell's law*, the ratio of the sines of the angles of incidence and refraction of a light ray is equal to the ratio of the refractive indices between them (for example, air-water),

$$n_1 \sin\theta_1 = n_2 \sin\theta_2. \tag{20}$$

Squaring Eq. (20) on both sides, we get,

$$n_1^2 \sin^2\theta_1 = n_2^2 \sin^2\theta_2. \tag{21}$$

Differentiating the Eq. (21),

$$2n_1^2 \sin\theta_1 \cdot \cos\theta_1 \Delta\theta_1 = 2n_2^2 \sin\theta_2 \cdot \cos\theta_2 \Delta\theta_2. \tag{22}$$

Multiplying $\Delta\phi$ on both sides, we get,

$$n_1^2 \sin\theta_1 \cdot \cos\theta_1 \Delta\theta_1 \Delta\phi = n_2^2 \sin\theta_2 \cdot \cos\theta_2 \Delta\theta_2 \Delta\phi. \tag{23}$$

The element of solid angle in spherical coordinates is given by, $\Delta\Omega = \frac{\Delta A}{r^2} = \frac{(r\sin\theta\Delta\phi)(r\Delta\theta)}{r^2} = \sin\theta\Delta\theta\Delta\phi$, therefore,

$$\Delta\Omega_1 = \sin\theta_1 \Delta\theta_1 \Delta\phi. \tag{24}$$

$$\Delta\Omega_2 = \sin\theta_2 \Delta\theta_2 \Delta\phi. \tag{25}$$

Substituting Eqs. (24) and (25) in Eq. (23), we get,

$$n_1^2 \cos\theta_1 \Delta\Omega_1 = n_2^2 \cos\theta_2 \Delta\Omega_2. \tag{26}$$

The above equation is known as *Straubel's invariant* in geometric optics. According to Eq. (1), the spectral radiance is the measure of radiant power per unit area, per unit solid angle within a wavelength interval. Therefore, it can be rewritten as,

$$L_1 = \frac{\Delta\Phi_1}{\Delta A_1 \Delta\Omega_1 \Delta\lambda}. \tag{27}$$

$$L_2 = \frac{\Delta\Phi_2}{\Delta A_2 \Delta\Omega_2 \Delta\lambda}. \tag{28}$$

From the work of Fresnel, we can write the ratio of radiant powers of the respective mediums as equivalent to Fresnel transmittance '*t*'. Therefore, we can write,

$$t = \frac{\Delta\Phi_2}{\Delta\Phi_1}. \tag{29}$$

From the immersion optics,

$$\Delta A_1 = \Delta A \cos\theta_1. \tag{30}$$

$$\Delta A_2 = \Delta A \cos\theta_2. \tag{31}$$

Taking ratios of Eqs. (27) and (28),

$$\begin{gathered} \frac{L_2}{L_1} = \frac{\Delta\Phi_2\, \Delta A_1\, \Delta\Omega_1}{\Delta\Phi_1\, \Delta A_2\, \Delta\Omega_2}. \\ \frac{L_2}{L_1} = t\frac{\cos\theta_1 \Delta\Omega_1}{\cos\theta_2 \Delta\Omega_2}. \end{gathered} \tag{32}$$

Comparing Eqs. (26) and (32),

$$\frac{L_2}{L_1} = t\frac{n_2^2}{n_1^2}. \tag{33}$$

Equation (33) is known as $n^2$ *law for radiance*.

As we deal with the transfer of radiance from water (medium 1) to air (medium 2), then $L_1 = L_u$, $L_2 = L_w$ and $\tau = \tau_{w,a}$, $n_1 = n$ and $n_2 = n_a$, where $n_a$ is approximately equal to 1. Then,

$$L_w = \frac{t}{n^2} L_u. \tag{34}$$

where $t = 1\text{-}\rho$ and $t/n^2$ is the radiance transmittance $\tau$. The above form Eq. (34) is represented in Eq. (3) in the manuscript.

## Appendix B: *Calculation of particulate refractive index relative to seawater, $r_f$*

Particulate refractive index $r_f$ is not a direct measured quantity, however, it can be calculated indirectly from the existing models. We have calculated the $r_f$ using Eq. (21) of Sahu and Shanmugam [27]:

$$r_f = 1 + \left(\frac{P_1}{\tilde{b}_{bp}}\right)^{\frac{1}{2P_2}}. \tag{35}$$

**Table 2. Coefficients for the determination of $r_f$.**

| m | $a_m$ | $b_m$ | $c_m$ |
|---|---|---|---|
| 1 | 0.03182 | 0.00416 | 0.1514 |
| 2 | 0.10100 | 0.00372 | −0.6116 |

where, $P_m = a_m\gamma^2 + b_m\gamma + c_m$ ; $m = 1, 2$. $a_m$, $b_m$ and $c_m$ are the coefficients from Table 2; $\gamma$ can be obtained from two methods, (*i*) from the attenuation hyperbolic slope [36,37], or (*ii*) from the particle size distribution slope (PSD), $\gamma = \xi - 3$ [23]. Petzold average-particle phase function can be used as a substitute to the backscattering ratio $\tilde{b}_{bp}$ because each phase function has a backscatter fraction of 0.0183 [38].

## Funding

Department of Science and Technology (DST) through the Networked Project on Big Data Analytics-Hyperspectral Data (OEC1617130DSTXPSHA); Research Management Fund (RMF) from IIT Madras.

## Acknowledgments

We sincerely thank the three anonymous reviewers for their helpful and constructive comments.